Design, Synthesis, and Biological Activity of Hybrid Compounds between Uramustine and DNA Minor Groove Binder Distamycin A

Pier Giovanni Baraldi,*,† Romeo Romagnoli,† Antonio Entrena Guadix,‡ Maria Josè Pineda de las Infantas,‡ Miguel Angel Gallo,‡ Antonio Espinosa,‡ Alberto Martinez,‡ John P. Bingham,§ and John A. Hartley§

Dipartimento di Scienze Farmaceutiche, Università di Ferrara, 44100 Ferrara, Italy, Departamento de Quimica Organica y Farmaceutica, Facultad de Farmacia, Campus de Cartuja s/n, 18071 Granada, and Cancer Research UK Drug−DNA Interactions Research Group, Department of Oncology, Royal Free and University College Medical School, UCL, 91 Riding House Street, London WIW 7BS, U.K.

Received November 28, 2001

The design, synthesis, characterization, DNA binding properties, and cytotoxic activity of a novel series of hybrids, namely, a molecular combination of the natural antibiotic distamycin A and the antineoplastic agent uramustine, are reported, and the structure−activity relationships are discussed. This homologous series **29**−**34** consisted of the minor groove binder distamycin A joined to uramustine (uracil mustard) by suitable aliphatic carboxylic acid moieties containing a flexible polymethylene chain that is variable in length [$(CH_2)_n$, where $n = 1-6$). All the hybrid compounds in this series exhibit enhanced activity compared to both distamycin A and uramustine derivatives **22**−**27** used for conjugation, giving IC_{50} values in the range 7.26−0.07 μM following a 1 h exposure of human leukemic K562 cells, with maximal activity shown when $n = 6$. The distance between the uramustine and distamycin frame is crucial for the cytotoxicity, with compounds having linker lengths of four to six being at least 20-fold more cytotoxic than liker lengths one to three. Taq polymerase stop experiments demonstrated selective covalent binding of uramustine−distamycin hybrids to A/T rich DNA sequences, which was again more efficent with compounds **32**−**34** with a longer linker length. Two consequences can be derived from our study: (a) the distamycin moiety directs binding to the minor groove of A/T rich DNA sequences and, consequently, is responsible for the alkylation regioselectivity found in footprinting studies; (b) the higher flexibility due to a longer linker between the distamycin and uracil moieties allows the formation of complexes with the mustard moiety situated more deeply in the minor groove and, hence, with better alkylating properties.

Introduction

The putative mode of action of many antitumor agents involves DNA damage; however, most of the DNA-interacting agents have only a limited degree of sequence specificity, which implies that they may hit all the cellular genes. DNA minor groove binders are one of the most widely studied class of antitumor agents, and the recent increased interest in this group of compounds stems from their ability to interact in a sequence-selective fashion at quite long DNA binding sites, inducing a range of mutations from simple base sequence changes to deletions.[1−3]

The prototype of this class of compounds is distamycin A (**1**), a natural antibiotic isolated in 1962 in the Farmitalia laboratories from the fermentation broth of *Streptomyces distallicus*.[4−6] It is characterized by an oligopeptidic pyrrolocarbamoyl frame ending with an amidino moiety. Distamycin A is able to interact reversibly to the minor groove of double-helical DNA, recognizing sequences containing at least four AT base pairs. A combination of hydrogen bonding, van der Waals contacts with the walls of the minor groove, and electrostatic interactions between the cationic amidine edge and the DNA contribute to the high affinity for ligand binding.[7−10] Despite its high DNA binding affinity, distamycin A shows limited cytotoxicity and only modest antitumor activity, which improved when alkylating moieties (such as nitrogen mustard, aziridine, oxirane, halogen acetyl, and α-halogen acrylic functions) were linked to the amino group of the desformyl derivative of distamycin A, disclosing the possibility of obtaining cytotoxic and antitumor agents by combining a chemically reactive moiety with a DNA binding frame.[11−14]

Nitrogen mustards are among the DNA alkylating agents most widely used in chemotherapy.[15] Uramustine (uracil mustard) **2** is an inexpensive oral alkylating agent that has been effective in the treatment of patients with lymphosarcoma,[16,17] chronic lymphatic leukaemia,[18] and thrombocythemia.[19] Uramustine interacts in GC-rich regions, being able to alkylate guanine-*N*7 in 5′-Py*G*CC-3′ (Py = pyrimidine) sequences.[20−22]

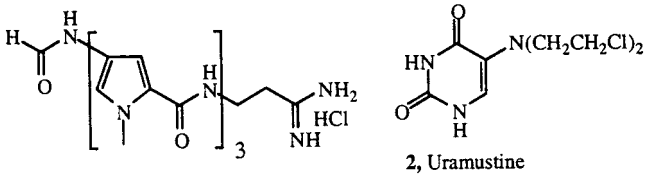

1, Distamycin A **2,** Uramustine

The concept of using a DNA minor groove binder, such

* To whom correspondence should be addressed. Phone: +39-(0)-532-291293. Fax: +39-(0)532-291296. E-mail: pgb@ifeuniv.unife.it.
† Università di Ferrara.
‡ Universidad de Granada.
§ University College London.

10.1021/jm011113b CCC: $22.00
Published on Web 07/13/2002

as distamycin A or its modified analogues, as a vector to deliver an alkylating function has been described in the literature.[23,24] In many cases, these hybrid compounds failed to present significant advantages in terms of activity, and in some cases, these derivatives even lost antitumor activity. For example, hybrids between distamycin and simplified enedyne moiety[25] or intercalating chromophores, where the latter were exemplified by anilinoacridine,[26] ellipticine,[27] and anthraquinone[28] derivatives, have proved so far to be particularly unsuccessful. In contrast, hybrids between minor groove binders, exemplified by the combination of distamycin with Hoechst 33258,[29] anthramycin,[30−33] and the alkylating moiety of the antitumor antibiotic CC-1065,[34−36] have recently been reported and represent a success of the hybrid drug approach.

In this article, we report the synthesis and in vitro antitumor activity of a novel series of distamycin conjugates, where the N-terminal pyrrole residue of the distamycin A is linked to uramustine by a different spacer (i.e., a polymethylene chain of varying length). These derivatives differed in the number of methylene units (one to six) between the N-terminal amino group of distamycin and the uracil moiety. A flexible polymethylene spacer was chosen, allowing the nitrogen mustard of uramustine to interact more closely with the DNA target. An enhanced DNA binding affinity and selectivity, along with increased biological activity, are the potential advantages of hybrid molecules of this type.

Chemistry

The synthetic route followed for the synthesis of derivatives **29**−**34** is outlined in Scheme 1, and the synthesis of these hybrid compounds required the preparation of uramustine derivatives **22**−**27** bearing a carboxylic acid moiety to provide a point of attachment of the carrier deformyldistamycin A **28**. One of the most adaptable and useful synthetic strategies for the present purposes is that previously reported by Martinez and co-workers,[37] where the syntheses of derivatives **23** and **24** were described.

Starting from the 5-nitro-1*H*-pyrimidine-2,4-dione **3**, it was alkylated at the N1 position, using commercially available *ω*-bromoesters, to give the nitrouracil esters **4**−**9** (Scheme 1) in poor yield. This was likely due to the prevalent and concomitant N3 alkylation. The subsequent reduction by catalytic hydrogenation over 10% Pd/C in 2-methoxyethanol afforded the aminouracils **10**−**15**, which were converted in acceptable yield to the corresponding *N*,*N*-bis(2-hydroxyethyl)aminouracil derivatives **16**−**21**, respectively, by reaction with a large excess of ethylene oxide in acetic acid. Subsequent treatment with phosphorus oxytrichloride ($POCl_3$) afforded the corresponding dichloronitrogen mustards, which were transformed into the desired uracilalkanoic acids **22**−**27** by acid hydrolysis. These latter compounds were in turn condensed with *N*-deformyldistamycin (**28**) in dry DMF using 1-ethyl-3[3-dimethylamino)propyl]-carbodiimide (EDC) as coupling agent to afford the conjugates **29**−**34** in good yield after purification by silica gel flash chromatography.

Scheme 1[a]

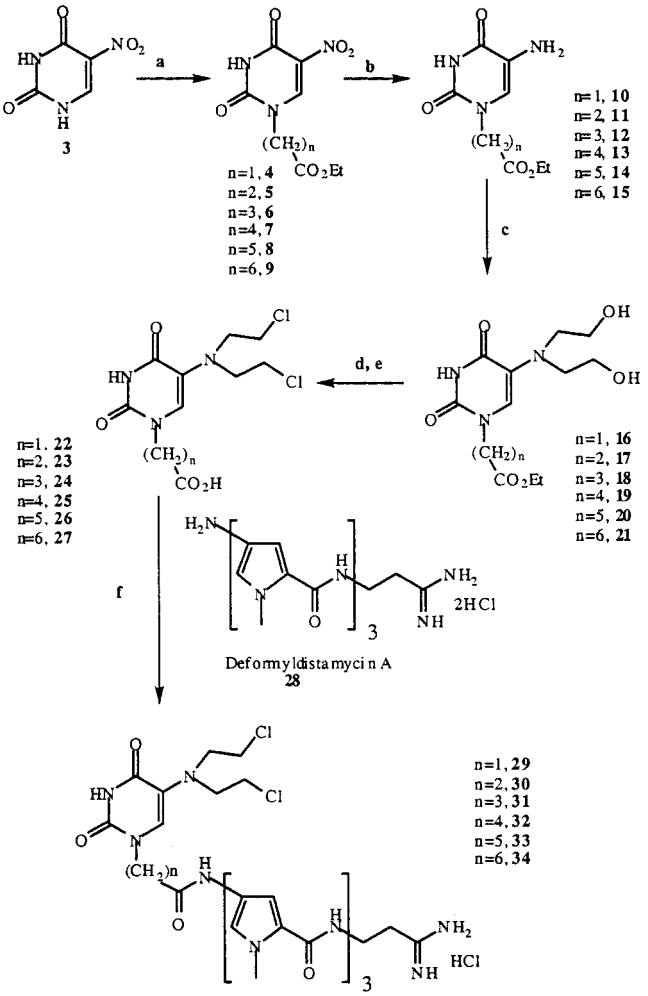

[a] Reagents: (a) NaH, DMF, then $Br(CH_2)_nCO_2Et$ with $n = 1-6$; (b) H_2, 10% Pd/C, 2-methoxyethanol; (c) ethylene oxide, CH_3CO_2H/H_2O; (d) $POCl_3$; (e) 37% HCl in water, reflux; (f) **9**, Hunig's base (DIPEA), EDC, DMF, 24 h, room temp.

Results and Discussion

In Vitro Antitumor Activity. The effects of the seven synthesized hybrid compounds **29**−**34** and uramustine alkanoic acids **22**−**27** on tumor cell growth were evaluated in vitro by using the human chronic myeloid leukaemia K562 cell line and compared to the effects of natural product distamycin A **1** and uramustine **2**. The antiproliferative effect was assayed by determing the IC_{50} values after 4 days of cell culture following a 1 h exposure, and the results are shown in Table 1.

Only the uracil acetic acid **22**, with an IC_{50} value of 33.50 μM, showed weak cytotoxic activity, while the other alkanoicuracil derivatives **23**−**27** showed no significant activity on K562 cell proliferation even at doses of 100 μM. Uramustine gave an IC_{50} of 5.1 μM, and therefore, the alkanoic side chain causes a significant change in the biological properties of uramustine.[37]

As a result of the linking of distamycin and uramustine via the polymethylene linkers [$(CH_2)_n$, with $n = 1-6$], the antitumor activity was markedly enhanced relative to that of the parent compounds distamycin A ($IC_{50} > 100$ μM) and uramustine derivatives **22**−**27** alone. Compounds **29**−**31** with methylene linker lengths

Table 1. In Vitro Activity of Distamycin A, Uramustine, and Compounds **22**−**27** and **29**−**34** against K562 Human Leukemia Cell Line[a]

compd	in vitro $IC_{50} \pm$ SEM (μM)	compd	in vitro $IC_{50} \pm$ SEM (μM)
distamycin A	>100	**27**	>100
uramustine	5.1 ± 0.6	**29**	4.06 ± 1.03
22	33.50 ± 9.4	**30**	2.54 ± 2.23
23	>100	**31**	7.26 ± 5.88
24	>100	**32**	0.11 ± 0.02
25	>100	**33**	0.14 ± 0.05
26	>100	**34**	0.07 ± 0

[a] IC_{50} = 50% inhibitory concentration as the mean ± SEM. The mean is from dose−response curves of at least three experiments.

of one to three, respectively, gave similar IC_{50} values in the low micromolar range following a 1 h drug exposure. When the methylene linker length was increased (compounds **32**−**34**, $n = 4-6$, respectively), the in vitro activity was increased by at least 20-fold with IC_{50} values in the range 0.07−0.14 μM. Compound **34**, with the longest linker length in the series, was the most active compound with an IC_{50} value greater than 1000 times lower than that for distamycin in this same screen. With the exception of **31**, all linked compounds were more active than uramustine. In summary, there was a large increase in cytotoxicity across the homologous series that cannot be explained entirely by changes in mustard reactivity and may be related to alteration of the orientation of the mustard with respect to the DNA.

DNA Sequence Specificity. DNase I footprinting experiments showed that **29**−**34** gave footprints at A/T rich sequences with a noncovalent binding specificity identical to that observed for distamycin and tallimustine (data not shown). Compounds **32**−**34** were more effective at producing footprints than **29**−**31**. The alkanoic uramustine derivatives **22**−**27** produced no evidence of footprinting at any concentration tested (data not shown).

Sites of sequence-specific DNA alkylation produced by the compounds **29**−**34** tested were determined using the Taq polymerase stop assay[38a] (Figure 1). At a concentration of 10 μM, the hybrid molecules **29**−**31** gave clear evidence of alkylation with several sites of alkyation observed in the sequence analyzed (Figure 1A). The patterns of covalent modification were distinct from that of cisplatin, which bound primarily at GG sequences within the sequence. Compounds **32**−**34** gave a comparable level of alkylation to **29**−**31** but at a 10-fold lower dose (Figure 1B). Derivatives **22**−**27** did not give significant alkylation at comparable doses (data not shown). Further analysis of the sites of covalent modification for compounds **29**−**34** revealed three major sites of sequence-specific alkylation, labeled 1, 2, and 3 in Figure 1. These corresponded to the sequences 5′-TTTTTG, GAAAAA, and TTTTTA, respectively. All six derivatives bound at these sequences, but the relative extent of alkylation at these sites differed between compounds.

Alkylation at purine-*N*3 in the DNA minor groove was confirmed using a thermal cleavage-based sequencing assay.[38b] The results for compound **33** are shown in Figure 2. Cleavage is observed at sites corresponding

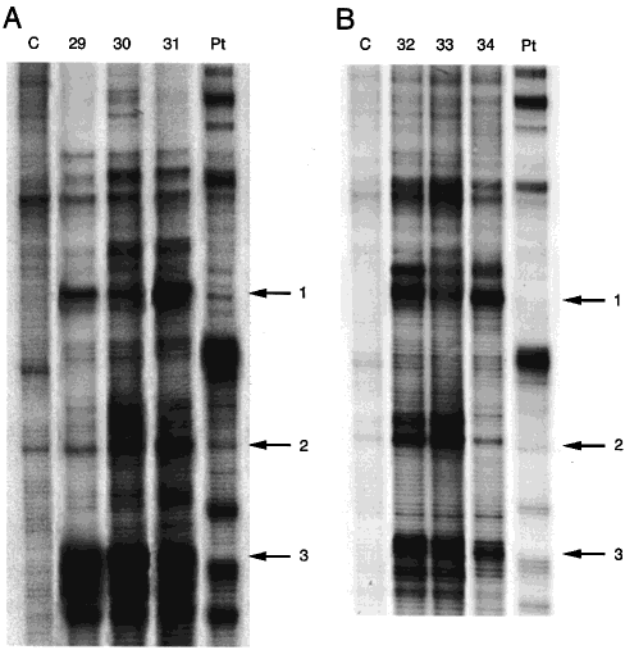

Figure 1. DNA sequence selective alkylation by **29**−**34** using the Taq polymerase stop assay. The doses of **29**−**31** and cisplatin (Pt) are 10 μM for 1 h, and the doese of **32**−**34** are 1 μM for 1 h. Lane C is a control lane from untreated DNA. Parts A and B show the same representative region from two different gels, and the three major sites of sequence-selective alkylation by **29**−**34** are indicated by arrows. The sequence at sites 1, 2, and 3 are 5′-TTTTTG, AAAACG, and TTTTTTA, respectively.

to sites 1−3 observed using the Taq polymerase stop assay. In contrast, no cleavage is observed with uramustine at the same concentrations. This is consistent with known alkylation of this compound at guanine-*N*7 sites in the major groove, which would not be detected using the thermal cleavage conditions employed.

Molecular Modeling Studies. Molecular modeling of the distamycin hybrid compounds performed over the three DNA sequences (see Experimental Section for details) demonstrates that in all cases, there exists a hydrogen bond pattern formed between the NH moieties of the ligand and the adenine N3 and thymine O2 atoms that is similar to the pattern described for distamycin.[7] Figure 3 shows a schematic representation of the hydrogen bond pattern in the three studied sequences.

For each DNA sequence, two types of conformation can be found, depending on the orientation of the uracil 5-substituent. In the first one, the uracil is inserted in the DNA minor groove with the 5-substituent oriented toward the bottom of the minor groove (inward conformation), while in the second, the uracil still lies in the minor groove but the 5-substituent is oriented away from the minor groove (outward conformation). Figure 4 shows, as an example, both types of conformation for compound **34** inserted into the 5′-TCGATTTTTGTGAT-3′ DNA sequence. The hydrogen bond patterns due to the distamycin moiety are clearly visible in the outward conformation.

The number and the stability of each type of conformation depended on the length of the linker between the distamycin and uracil fragments. In compounds with one or two carbon atoms (**29** and **30**), the smaller flexibility of the molecule increased the number and the

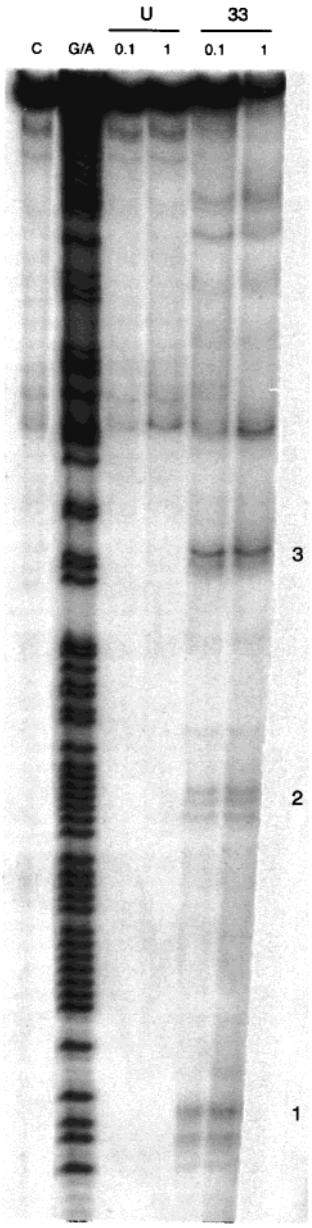

Figure 2. Thermal cleavage assay for **33** and uramustine (U) at 0.1 and 1 μM. Lane C is a control lane for untreated DNA. G/A is a formic acid purine specific sequencing lane. Sites 1−3 correspond to the main sites of alkylation observed using the Taq polymerase stop assay (Figure 1).

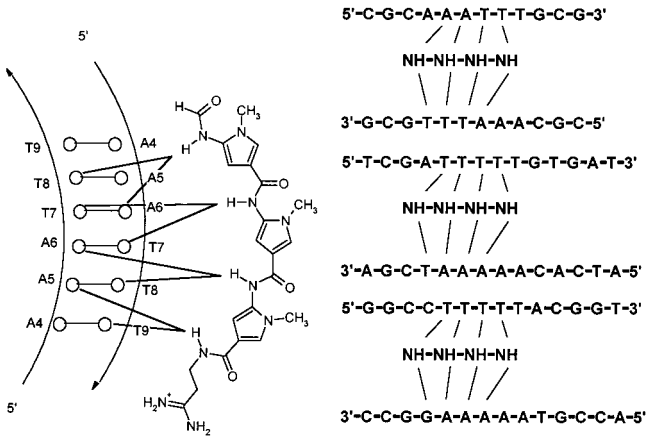

Figure 3. Left: schematic representation of the hydrogen bond pattern formed between NH amide moieties of distamycin and the DNA bases in a fragment of the 5′-CGCAAATTTGCG-3′ sequence. Circles represent the N3 and O2 atoms of adenine and thymine, which act as hydrogen bond acceptors. Right: alignment of the three sequences studied.

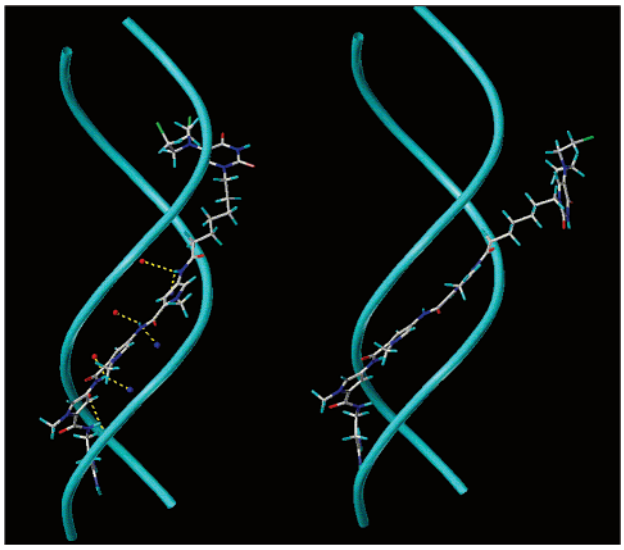

Figure 4. Inward (left) and outward (right) conformations of **34** complexed with 5′-TCGATTTTTGTGAT-3′ DNA sequence. In all complexes, there exists a hydrogen bond pattern due to the distamycin moiety, which has been shown as an example in the inward conformation.

stability of the outward conformation. For example, for **29** inserted in the 5′-TCGATTTTTGTGAT-3′ DNA sequence, 12 outward conformations were more stable than the less energetic inward conformation. In contrast, in compounds **33** and **34**, the inward conformation was preferred. In any case, however, the energy difference between both types of conformation is not high (3−5 kcal/mol, data not shown).

In the inward conformation only, the mustard moiety is in the appropriate orientation to allow efficient alkylation of one or more DNA bases. Compounds **33** and **34** in which the inward conformation is more stable show higher alkylation and cytotoxicity than **29** and **30**, where the outward conformation is more stable. Furthermore, in compounds **33** and **34**, the mustard moiety is situated more deeply in the minor groove, near a guanine moiety, and hence, the alkylation could take place more easily. Figure 5 shows a comparative view of the inward complex of both **29** (red) and **34** (blue) inserted in the three DNA sequences studied. In each case, the distance between the N3 position of the purine and one of the CH_2Cl groups of the mustard moiety is shorter in the ligand with a longer linker.

Conclusions

In conclusion, the longer-chain-length compounds **32**−**34** are more active than **29**−**31**, where compound **34** was the most reactive compound (IC_{50} = 70 nM). All these synthesized hybrids **29**−**34** showed an activity superior to that of uramustine derivatives **22**−**27** used for conjugation, and they were all found to be active as DNA alkylating agents. Nevertheless, the hybrid approach in this case has proved so far to be particularly advantageous in terms of activity and represents an important model for the design of new cytotoxic minor groove binders, having disclosed the possibility of obtaining

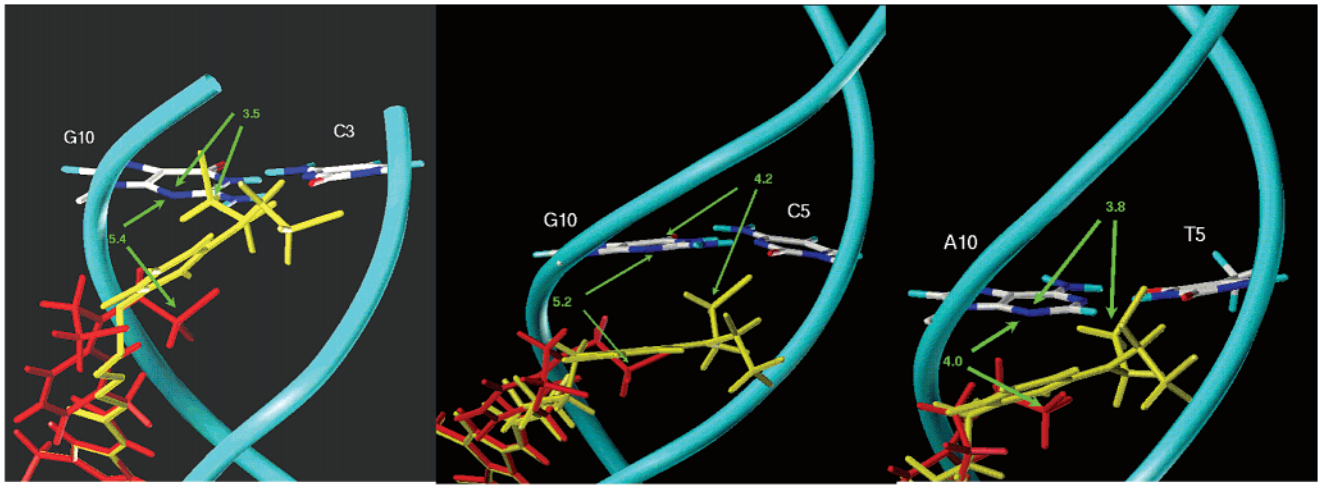

Figure 5. Comparative views of the inward complexes of **29** (red) and **34** (yellow) inserted into 5′-CGCAAATTTGCG-3′ (left), 5′-TCGATTTTTGTGAT-3′ (center), and 5′-GGCCTTTTTACGGT-3′ (right) DNA sequences. In **34**, the mustard moiety is situated deeply in the minor groove and a shorter distance from the N3 atom of the purine (G10 or A10), conferring better alkylating properties to the complex.

potent agents by combining moieties of mild cytotoxic activity with a DNA binding frame derived from distamycin A, acting as a sequence-selective vector. Also, in this case the interaction with DNA tends to be dominated by the minor groove binding moiety distamycin A. In fact, hybrids **29**−**34** bind to the minor groove with preferential interaction with AT-rich sequences. The relatively higher cytotoxicity of hybrid **34**, which has a longer spacer than the other hybrids, supports the idea that a proper length of spacer is important to achieve good binding potency of the hybrid molecule with the floor of the DNA minor groove while preserving optimal positioning of the mustard for DNA alkylation capability. Improved transportation of the compounds into the cells due to the increased lipophilicity may also play arole, since the longer-chain compounds **32**−**34** are more cytotoxic.

Efforts to further clarify and define these results are under study in our laboratories, including (a) structural studies, such as DNase I footprinting experiments performed using molecular probes mimicking a variety of promoter sequences involved in cell-cycle progression and neoplastic transformation, and (b) functional studies, such as gel shift and in vitro transcription.

Experimental Section

Chemical Materials and Methods. General Procedure. All reactions were carried out under an inert atmosphere of argon, unless otherwise described. Standard syringe techniques were applied for transferring dry solvents. Reaction courses and product mixtures were routinely monitored by TLC on silica gel (precoated F_{254} Merck plates) and visualized with aqueous $KMnO_4$. ^{1}H NMR spectra were recorded in the given solvent with a Bruker AC 200 spectrometer. Chemical shifts (δ) are given in parts per million (ppm) upfield from tetramethylsilane. The splitting pattern abbreviations are as follows: s (singlet), d (doublet), dd (double dublet), t (triplet), br (broad), and m (multiplet). Melting points (mp) were determined on a Buchi−Tottoli apparatus and are uncorrected. All products reported showed ^{1}H NMR spectra that are in agreement with the assigned structures. Elemental analyses were conducted by the Mycroanalytical Laboratory of the Chemistry Department of the University of Ferrara. All compounds obtained commercially were used without further purification. Organic solutions were dried over anhydrous Na_2SO_4. Dry DMF was distilled from calcium chloride and stored over molecular sieves (3 Å). In high-pressure hydrogenation experiments, a Parr shaker on a high-pressure autoclave was used.

General Procedure for the Synthesis of Compounds 4−9. To a well-stirred cooled 2 M solution of sodium hydride (1.5 equiv) in dry DMF was added dropwise a 2.5 M DMF solution of 5-nitrouracil **3** (1 equiv), followed by the addition of the suitable ω-bromoester (1.6 equiv) after 1 h at 100 °C and cooling with a ice−water bath. The solution was stirred for 24 h at room temperature and concentrated under reduced pressure. The resulting residue was dissolved in EtOAc and washed with water (twice). The organic layer was dried on Na_2SO_4 and concentrated under vacuum, and the residue was purified by silica gel flash chromatography (eluent AcOEt/petroleum ether, 1:1).

Ethyl *ω*-*N*1-[5-nitro-2,4-(1*H*,3*H*)pyrimidinedione]acetate (4): white solid; 186 mg (24% yield); mp 209 °C. ^{1}H NMR (CD_3COCD_3): δ 1.72 (t, 3H, J = 7.2 Hz), 4.72 (q, 2H, J = 7.0 Hz), 5.29 (s, 2H), 9.67 (s, 1H), 11.4 (bs, 1H). ^{13}C NMR (CD_3COCD_3): δ 13.52, 49.64, 61.77, 118.46, 133.43, 150.11, 154.21, 167.10. MS (EI) m/z: 243 (M^+), 171, 156, 127, 83 (100), 56, 53. Anal. ($C_8H_9N_3O_6$): C, H, N.

Ethyl *ω*-*N*1-[5-nitro-2,4-(1*H*,3*H*)pyrimidinedione]propanoate (5): white solid; 147 mg (18% yield); mp 172 °C (lit.[10] 170−171 °C). ^{1}H NMR (DMSO): δ 1.17 (t, 3H, J = 7.2 Hz), 2.66 (t, 2H, J = 6.6 Hz), 4.09 (m, 4H), 9.26 (s, 1H), 12.04 (s, 1H). ^{13}C NMR (DMSO): δ 13.46, 31.68, 44,86, 59.82, 124.07, 148.77, 150.89, 154.53, 170.15. MS (EI) m/z: 257 (M^+), 212, 183, 127, 99, 83, 73, 55 (100). Anal. ($C_9H_{11}N_3O_6$): C, H, N.

Ethyl *ω*-*N*1-[5-nitro-2,4-(1*H*,3*H*)pyrimidinedione]butanoate (6): white solid; 180 mg (21% yield); mp 140 °C (lit.[10] 130−132 °C). ^{1}H NMR (DMSO): δ 1.16 (t, 3H, J = 7 Hz), 1.90 (m, 2H), 2.39 (t, 2H, J = 7.4 Hz), 3.87 (t, 2H, J = 6.8 Hz), 4.02 (q, 2H, J = 7.2 Hz), 9.26 (s, 1H), 11.99 (bs, 1H). ^{13}C NMR (DMSO): δ 13.54, 23.11, 29.85, 48.09, 59.45, 124.46, 148.92, 150.27, 154.54, 171.82. MS (EI) m/z: 272 (M + 1), 242, 196, 123 (100), 115, 87. Anal. ($C_{10}H_{13}N_3O_6$): C, H, N

Ethyl *ω*-*N*1-[5-nitro-2,4-(1*H*,3*H*)pyrimidinedione]pentanoate (7): white solid; 235 mg (26% yield); mp 133 °C. ^{1}H NMR ($CDCl_3$): δ 1.26 (t, 3H, J = 7.2 Hz), 1.72 (m, 4H), 2.4 (t, 2H, J = 7.0 Hz), 3.94 (t, 2H, J = 6.8 Hz), 4.15 (q, 2H, J = 7.2 Hz), 8.78 (s, 1H), 8.85 (bs, 1H). ^{13}C NMR ($CDCl_3$): δ 14.20, 21.41, 28.42, 33.31, 50.26, 60.72, 125.41, 148.79, 148.79, 154.20, 172.97. MS (EI) m/z: 286 (M + 1 − 100), 267, 240, 210, 137, 129, 55. Anal. ($C_{11}H_{15}N_3O_6$): C, H, N.

Ethyl *ω*-*N*1-[5-nitro-2,4-(1*H*,3*H*)pyrimidinedione]hexanoate (8): white solid; 238 mg (17% yield); mp 125 °C. ^{1}H NMR ($CDCl_3$): δ 1.25 (t, 3H, J = 7.2 Hz), 1.41 (m, 2H), 1.73 (m,

4H), 2.33 (t, 2H, $J = 7.1$ Hz), 3.93 (t, 2H, $J = 7.3$ Hz), 4.13 (q, 2H, $J = 7.2$ Hz), 8.77 (s, 1H), 9.14 (s, 1H). ^{13}C NMR ($CDCl_3$): δ 14.22, 24.02, 25.63, 28.67, 33.74, 50.4, 60.52, 125.36, 148.61, 148.84, 154.17, 173.42. MS (EI) *m/z*: 300 (M + 1), 270, 254, 224, 151 (100), 143, 123. Anal. ($C_{12}H_{17}N_3O_6$): C, H, N.

Ethyl *ω*-*N*1-[5-nitro-2,4-(1*H*,3*H*)pyrimidinedione]heptanoate (9): white solid; 271 mg (27% yield); mp 108 °C. ^{1}H NMR ($CDCl_3$): δ 1.25 (t, 3H, $J = 7.0$ Hz), 1.38 (m, 4H), 1.70 (m, 4H), 2.31 (t, 2H, $J = 7.2$ Hz), 3.91 (t, 2H, $J = 7.3$ Hz), 4.13 (q, 2H, $J = 7.1$ Hz), 8.77 (s, 1H), 9.14 (bs, 1H). ^{13}C NMR ($CDCl_3$): δ 14.24, 24.47, 25.89, 28.36, 28.81, 34.00, 50.55, 60.39, 125.33, 148.62, 148.78, 154.16, 176.63. MS (EI) *m/z*: 314 (M + 1), 295, 158, 109, 83, 69, 55 (100). Anal. ($C_{13}H_{19}N_3O_6$): C, H, N.

General Procedure for the Synthesis of Compounds 10−15. A solution of nitrouracil ester **4**−**9** (5 mmol) and 10% Pd/C (150 mg) in 2-methoxyethanol (20 mL) was hydrogenated at room temperature and a pressure of 55 psi until TLC analysis indicated complete reduction of the starting material (2 h). The catalyst was removed by filtration, the filtrate was concentrated, and the residue gave a white solid material consisting of **10**−**15**, which was kept under vacuum until ready for use in the next step.

Ethyl 2-[5-amino-2,4-(1*H*,3*H*)pyrimidinedione]acetate (10): white solid; 93% yield; mp 165 °C. ^{1}H NMR (CD_3OD): δ 1.27 (t, 3H, $J = 7.2$ Hz), 4.22 (q, 2H, $J = 7.2$ Hz), 4.44 (s, 2H), 6.88 (s, 1H). ^{13}C NMR (CD_3OD): δ 14.40, 50.01, 62.79, 124.06, 144.5, 151.61, 163.18, 169.71. MS (EI) *m/z*: 213 (M^+), 140, 97, 86, 69, 55, 42 (100). Anal. ($C_8H_{11}N_3O_4$): C, H, N.

Ethyl 3-[5-amino-2,4-(1*H*,3*H*)pyrimidinedione]propanoate (11): white solid; 92% yield; mp 120−122 °C. ^{1}H NMR (CD_3OD): δ 1.24 (t, 3H, $J = 7.2$ Hz), 2.72 (t, 2H, $J = 6.6$ Hz), 3.94 (t, 2H, $J = 6.7$ Hz), 4.14 (q, 2H, $J = 7.2$ Hz), 6.98 (s, 1H). ^{13}C NMR (DMSO): δ 14.44, 34.12, 45.79, 61.92, 124.48, 144.0, 150.30, 163.14, 172.72. FAB (EM high resolution) calculated for $C_9H_{13}N_3O_4Na$ [M + Na]$^+$: 250.0804. Found: 250.0804. Anal. ($C_9H_{13}N_3O_4$): C, H, N.

Ethyl 4-[5-amino-2,4-(1*H*,3*H*)pyrimidinedione]butanoate (12): white solid; 93% yield; mp 175 °C. ^{1}H NMR (CD_3OD): δ 1.24 (t, 3H, $J = 7.2$ Hz), 1.95 (m, 2H), 2.39 (t, 2H, $J = 7.1$ Hz), 3.72 (t, 2H, $J = 4.9$ Hz), 4.10 (q, 2H, $J = 4.9$ Hz), 7.05 (s, 1H). ^{13}C NMR (CD_3OD): δ 14.55, 22.92, 32.10, 44,94, 61.64, 125.77, 144.65, 152.99, 161.29, 172.98. MS (EI) *m/z*: 242 (M + 1) 196, 115, 112, 95, 86, 73, 61, 57. Anal. ($C_{10}H_{15}N_3O_4$) C, H, N.

Ethyl 5-[5-amino-2,4-(1*H*,3*H*)pyrimidinedione]pentanoate (13): white solid; 90% yield; mp 150 °C. ^{1}H NMR (DMSO): δ 1.16 (t, 3H, $J = 7.1$ Hz), 1.50 (m, 4H), 2.31 (m, 2H), 3.33 (m, 2H), 4.03 (q, 2H, $J = 7.1$ Hz), 7.0 (s, 1H), 10.58 (s, 1H), 12.91 (s, 2H). ^{13}C NMR (DMSO): δ 14.03, 21.44, 25.37, 32.97, 43.29, 59.61, 125.0, 143.68, 150.65, 158.66, 172.70. MS (EI) *m/z*: 256 (M + 1), 210, 100, 57, 55. Anal. ($C_{11}H_{17}N_3O_4$): C, H, N.

Ethyl 6-[5-amino-2,4-(1*H*,3*H*)pyrimidinedione]hexanoate (14): white solid; 93% yield; mp 176 °C. ^{1}H NMR (CD_3OD): δ 1.23 (t, 3H, $J = 7.1$ Hz), 1.37 (m, 2H), 1.66 (m, 4H), 2.33 (t, 2H, $J = 7.3$ Hz), 3.75 (t, 2H), 4.10 (q, 2H, $J = 7.2$ Hz), 7.0 (s, 1H). ^{13}C NMR (CD_3OD): δ 14.64, 25.76, 27.20, 27.39, 34.97, 44.91, 61.49, 128.76, 144.69, 152.91, 161.38, 175.48. MS (EI) *m/z*: 270 (M + 1), 224, 140, 114, 69, 61, 57. Anal. ($C_{12}H_{19}N_3O_4$): C, H, N.

Ethyl 7-[5-amino-2,4-(1*H*,3*H*)pyrimidinedione]heptanoate (15): white solid; 97% yield; mp 98 °C. ^{1}H NMR (CD_3OD): δ 1.23 (t, 3H, $J = 7,1$ Hz), 1.35 (m, 4H), 1.63 (m, 4H), 2.3 (t, 2H, $J = 7,3$ Hz), 3.66 (t, 2H, $J = 7.1$), 4.10 (q, 2H, $J = 7.1$ Hz), 6.92 (s, 1H). ^{13}C NMR (CD_3OD): δ 14.54, 25.83, 27.09, 29.70, 34.91, 49.13, 61.38, 123.96, 144.0, 151.37, 163.05, 175.45. MS (EI) *m/z*: 283 (M^+), 238, 140, 127 (100), 83, 69, 55, 41. Anal. ($C_{13}H_{21}N_3O_4$): C, H, N.

General Procedure for the Synthesis of Compounds 16−21. To a solution of aminoesters **10**−**15** (1 mmol) in a 25% aqueous solution of acetic acid (3 mL) cooled in a ice bath, cold ethylene oxide (0.6 mL, 11.36 mmol) was added. The reaction flask was sealed and allowed to reach room temperature overnight. After this time, the solution was cooled and neutralized with $NaHCO_3$ (1 g) to pH 7. The mixture was extracted with ethyl acetate (3 × 10 mL), and the organic layers were combined and dried (Na_2SO_4). The crude residue was purified by flash chromatography on silica gel using EtOAc/MeOH as eluent (9.5:0.5, 9:1, 8:2, and finally 7:3).

Ethyl 2-[5-bis(2-hydroxyethyl)amino-2,4-(1*H*,3*H*)pyrimidinedione]acetate (16): brown gum; 135 mg (45% yield). ^{1}H NMR (CD_3OD): δ 1.28 (t, 3H, $J = 7.0$ Hz), 3.12 (t, 4H, $J = 5.4$ Hz), 3.59 (t, 4H, $J = 5.4$ Hz), 4.22 (q, 2H, $J = 7.1$ Hz), 4.53 (s, 2H), 7.50 (s, 1H). ^{13}C NMR (DMSO): δ 14.43, 50.03, 57.01, 60.33, 62.94, 125.21, 141.82, 152.05, 165.47, 169.61. FAB (EM high resolution) calculated for $C_{12}H_{19}N_3O_6Na$ [M + Na]$^+$: 324.1171. Found: 324.1171. Anal. ($C_{12}H_{19}N_3O_6$): C, H, N.

Ethyl 3-[5-bis(2-hydroxyethyl)amino-2,4-(1*H*,3*H*)pyrimidinedione]propanoate (17): brown gum; 180 mg (57% yield). ^{1}H NMR (CD_3OD): δ 1.27 (t, 3H, $J = 7.1$ Hz), 2.78 (t, 2H, $J = 6.5$ Hz), 3.15 (t, 4H, $J = 5.5$ Hz), 3.60 (t, 4H, $J = 5.5$ Hz), 4.00 (t, 2H, $J = 6.5$ Hz), 4.17 (q, 2H, $J = 7.1$ Hz), 7.52 (s, 1H). ^{13}C NMR (CD_3OD): δ 14.4, 33.8, 46.0, 56.9, 60.7, 62.0, 124.74, 142.3, 152.01, 165.16, 172.76. MS (EI) *m/z*: 338 (M + 23(Na)), 315 (M^+), 284, 254, 154, 73, 55. Anal. ($C_{13}H_{21}N_3O_6$): C, H, N.

Ethyl 4-[5-bis(2-hydroxyethyl)amino-2,4-(1*H*,3*H*)pyrimidinedione]butanoate (18): brown gum; 210 mg (63% yield). ^{1}H NMR (CD_3OD): δ 1.24 (t, 3H, $J = 7.2$ Hz), 1,98 (m, 2H), 2,39 (t, 2H, $J = 7.2$ Hz), 3.13 (t, 4H, $J = 5.5$ Hz), 3.57 (t, 4H, $J = 5.5$ Hz), 3,77 (t, 2H, $J = 6.9$ Hz), 4,11 (q, 2H, $J = 7.1$ Hz), 7.4 (s, 1H). ^{13}C NMR (CD_3OD): δ 14.53, 25.14, 31.82, 48.88, 56.81, 60.85, 61.71, 125.37, 141.45, 152.22, 165.05, 174.44. MS (EI) *m/z*: 330 (M + 1), 329 (M^+), 299 (100), 268, 180, 115, 87, 69. Anal. ($C_{14}H_{23}N_3O_6$): C, H, N.

Ethyl 5-[5-bis(2-hydroxyethyl)amino-2,4-(1*H*,3*H*)pyrimidinedione]pentanoate (19): brown gum; 140 mg (41% yield). ^{1}H NMR ($CDCl_3$): δ 1.25 (t, 3H, $J = 7.05$ Hz), 1.69 (m, 4H), 2.36 (t, 2H, $J = 6.5$ Hz), 3.16 (t, 4H, $J = 4.7$ Hz), 3.61 (t, 4H, $J = 4.7$ Hz), 3.72 (m, 2H), 4.13 (q, 2H, $J = 6.99$ Hz), 7.28 (s, 1H), 9.90 (s, 1H). ^{13}C NMR ($CDCl_3$): δ 14.23, 21.62, 28.23, 33.53, 48.44, 55.91, 59.77, 60.64, 123.80, 139.98, 150.26, 163.5, 173.44. MS (EI) *m/z*: 366 (M + 23(Na)), 343 (M^+), 312, 298, 186, 129, 72, 55. Anal. ($C_{15}H_{25}N_3O_6$): C, H, N.

Ethyl 6-[5-bis(2-hydroxyethyl)amino-2,4-(1*H*,3*H*)pyrimidinedione]hexanoate (20): brown gum; 155 mg (43% yield). ^{1}H NMR ($CDCl_3$): δ 1.26 (t, 3H, $J = 7.2$ Hz), 1.36 (m, 2H), 1.66 (m, 4H), 2.31 (t, 2H, $J = 7.1$ Hz), 3.17 (m, 4H), 3.60 (m, 4H), 3.72 (t, 2H, $J = 7$ Hz), 4.12 (q, 2H, $J = 7.2$ Hz), 7,35 (s, 1H). ^{13}C NMR ($CDCl_3$): δ 13.99, 20.83, 24.15, 28.42, 33.77, 48.34, 55.75, 59.59, 60.21, 123.48, 140.28, 150.29, 163.42, 173.45. FAB (EM high resolution) calculated for $C_{16}H_{27}N_3O_6Na$ [M + Na]$^+$: 380.1798. Found: 380.1796. Anal. ($C_{16}H_{27}N_3O_6$): C, H, N.

Ethyl 7-[5-bis(2-hydroxyethyl)amino-2,4-(1*H*,3*H*)pyrimidinedione]heptanoate (21): brown gum; 105 mg (28% yield). ^{1}H NMR (CD_3OD): δ 1.23 (t, 3H, $J = 6.9$ Hz), 1.36 (m, 4H), 1.64 (m, 4H), 2.31 (t, 2H, $J = 7.4$ Hz), 3.13 (t, 4H, $J = 5.5$ Hz), 3.56 (t, 4H, $J = 5.5$ Hz), 3.71 (t, 2H, $J = 7.1$ Hz), 4.1 (q, 2H, $J = 7.2$ Hz), 7.44 (s, 1H). ^{13}C NMR (CD_3OD): δ 25.83, 27.08, 29.67, 29.72, 34.91, 49.45, 56.85, 60.86, 61.40, 125.05, 141.83, 152.16, 164.97, 175.47. FAB (EM high resolution) calculated for $C_{17}H_{29}N_3O_6Na$ [M + Na]$^+$: 394.1954. Found: 394.1965. Anal. ($C_{17}H_{29}N_3O_6$): C, H, N.

General Procedure for the Synthesis of Compounds 22−27. compounds **16**−**21** (1 mmol) were cooled in an ice bath, and 2 mL of phosphorus oxychloride (20 mmol, 2 mL) were added dropwise. The solution was heated at 100 °C for 1 h, the solvent was evaporated under vacum, and then the residue was dissolved in EtOAc (8 mL) and washed with water (3 mL). The organic phase was dried (Na_2SO_4) and concentrated, and the crude product was used for the next reaction step without purification. The nitrogen mustard previously prepared starting from **16**−**21** was dissolved in 36% hydrochloric acid (4 mL) and heated at 100 °C for 3 h. The solution was cooled at room temperature, diluted with water (10 mL), and extracted with EtOAc (2 × 20 mL). The recombined organic phases were dried

(Na_2SO_4) and evaporated in vacuo, and the residue was purified by flash chromatography on silica gel using EtOAc as eluent.

2-[5-Bis(2-chloroethyl)amino-2,4-(1*H*,3*H*)pyrimidinedione]acetic acid (22): brown solid; 75 mg (24% yield); mp 158 °C. ^{1}H NMR (CD_3OD): δ 3.32 (m, 4H), 3.56 (m 4H), 4.36 (s, 2H), 7.41 (s, 1H). ^{13}C NMR (CD_3OD): δ 43.13, 51.22, 56.97, 123.78, 144.11, 152.50, 164.66. FAB (EM high resolution) calculated for $C_{10}H_{14}N_3O_4Cl_2$ $[M + H]^+$: 310.0361. Found: 310.0361. FAB (EM high resolution) calculated for $C_{10}H_{12}N_3O_4Na_2Cl_2$ $[M - H + Na_2]^+$: 354.0000. Found: 354.0002. Anal. ($C_{10}H_{13}N_3O_4Cl_2$): C, H, Cl, N.

3-[5-Bis(2-chloroethyl)amino-2,4-(1*H*,3*H*)pyrimidinedione]propionic acid (23): brown gum; 165 mg (51% yield); mp 200 °C (lit.[10] 206−300 °C). ^{1}H NMR (CD_3OD): δ 2.67 (t, 2H, J = 6.4 Hz), 3.31 (m, 4H), 3.55 (t, 4H, J = 6.8 Hz), 3.96 (t, 2H, J = 6.4 Hz), 7.52 (s, 1H). ^{13}C NMR (CD_3OD): δ 34.88, 43.17, 46.64, 56.89, 123.00, 144.20, 152.19, 164.54. FAB (EM high resolution) calculated for $C_{11}H_{15}N_3O_4NaCl_2$ $[M + Na]^+$: 346.0337. Found: 346.0338. Anal. ($C_{11}H_{15}N_3O_4Cl_2$): C, H, Cl, N.

4-[5-Bis(2-chloroethyl)amino-2,4-(1*H*,3*H*)pyrimidinedione]butanoic acid (24): brown solid; 170 mg (50% yield); mp 129 °C (lit.[10] 130−130.5 °C). ^{1}H NMR (CD_3OD): δ 1.97 (m, 2H), 2.37 (t, 2H, J = 7 Hz), 3.33 (t, 4H, J = 6.5 Hz), 3.56 (t, 4H, J = 6.6 Hz), 3.79 (t, 2H, J = 6.9 Hz), 7.46 (s, 1H). ^{13}C NMR (CD_3OD): δ 25.22, 31.64, 43.37, 49.05, 56.85, 123.53, 143.60, 152.40, 164.53, 176.49. FAB (EM high resolution) calculated for $C_{12}H_{17}N_3O_4NaCl_2$ $[M + Na]^+$: 360.0494. Found: 360.0491. Anal. ($C_{12}H_{17}N_3O_4Cl_2$): C, H, Cl, N.

5-[5-Bis(2-chloroethyl)amino-2,4-(1*H*,3*H*)pyrimidinedione]pentanoic acid (25): brown solid; 170 mg (49% yield); mp 95 °C. ^{1}H NMR ($CDCl_3$): δ 1.72 (m, 4H), 2.42 (t, 2H, J = 6.1 Hz), 3.35 (t, 4H, J = 6.1 Hz), 3.50 (t, 4H, J = 6.2 Hz), 3.75 (t, 2H, J = 6.3 Hz), 7.29 (s, 1H), 10.26 (s, 1H). ^{13}C NMR ($CDCl_3$): δ 21.31, 28.20, 33.25, 42.77, 48.52, 55.60, 121.79, 143.13, 150.74, 162.92, 178.24. FAB (EM high resolution) calculated for $C_{13}H_{19}N_3O_4NaCl_2$ $[M + Na]^+$: 374.0650. Found: 374.0652. Anal. ($C_{13}H_{19}N_3O_4Cl_2$): C, H, Cl, N.

6-[5-Bis(2-chloroethyl)amino-2,4-(1*H*,3*H*)pyrimidinedione]hexanoic acid (26): dark gum; 175 mg (48% yield); mp 105 °C. ^{1}H NMR (CD_3OD): δ 1.39 (m, 2H), 1.68 (m, 4H), 2.33 (t, 2H), 3.34 (t, 4H), 3.56 (t, 4H, J = 6.5 Hz), 3.74 (t, 2H, J = 7.1 Hz), 7.49 (s, 1H). ^{13}C NMR (CD_3OD): δ 25.58, 26.93, 29.62, 34.63, 43.38, 49.42, 56.81, 123.00, 143.78, 152.50, 164.49, 177.00. FAB (EM high resolution) calculated for $C_{14}H_{22}N_3O_4Cl_2$ $[M + H]^+$: 366.0987. Found: 366.0989. Anal. ($C_{14}H_{21}N_3O_4Cl_2$): C, H, Cl, N.

7-[5-Bis(2-chloroethyl)amino-2,4-(1*H*,3*H*)pyrimidinedione]heptanoic acid (27): brown solid; 200 mg (52% yield); mp 82 °C. ^{1}H NMR (CD_3OD): δ 1.38 (m, 4H), 1.61 (m, 2H), 1.68 (m, 2H), 2.29 (t, 2H, J = 7.4 Hz), 3.33 (t, 4H, J = 6.2 Hz), 3.55 (t, 4H, J = 6.5 Hz), 3.73 (t, 2H, J = 7.2 Hz), 7.48 (s, 1H). ^{13}C NMR (CD_3OD): δ 25.9, 27.1, 29.7, 34.8, 43.3, 49.3, 56.7, 123.26, 143.84, 152.31, 164.51, 177.71. FAB (EM high resolution) calculated for $C_{15}H_{23}N_3O_4NaCl_2$ $[M + Na]^+$: 402,0963. Found: 402.0972. Anal. ($C_{15}H_{23}N_3O_4Cl_2$): C, H, Cl, N.

General Procedure for the Synthesis of Compounds 30−34. To a stirred solution of *N*-deformyldistamycin A dihydrochloride **28** (526 mg, 1 mmol) in anhydrous DMF (5 mL) was added at 0 °C Hunig's base (192 μL, 1 mmol). After 5 min, **22**−**27** (1 mmol) and then EDCI (384 mg, 2 mmol) were added. The resulting mixture was stirred overnight as it warmed to room temperature, acidified with 20% HCl to pH 2, and then evaporated to dryness in vacum. The residue was dissolved in a small volume of MeOH, and then ethyl ether was added to precipitate the crude product as a brown solid. This procedure was repeated five times. The crude product was purified by coloumn chromatography (methylene chloride/methanol, 8:2).

3-[1-Methyl-4-[1-methyl-4-[1-methyl-4-[*N*1-[5-bis(2-chloroethyl)amino-2,4-(1*H*,3*H*)pyrimidinedione]acetylamino]-pyrrole-2-carboxamido]pyrrole-2-carboxamido]pyrrole-2-carboxamido]propionamidine hydrochloride (29): yellow solid; 485 mg (62% yield); mp 220 °C. ^{1}H NMR (DMSO): δ 2.63 (t, 2H, J = 6.5 Hz), 3.27 (t, 4H, J = 6.6 Hz), 3.49 (m, 2H), 3.58 (t, 4H, J = 6.8 Hz), 3.80 (s, 9H), 4.45 (s, 2H), 6.93 (s, 1H), 6.96 (s, 1H), 7.04 (s, 1H), 7.14 (s, 1H), 7.20 (s, 1H), 7.24 (s, 1H), 7.46 (s, 1H), 8.27 (t, 1H), 8.82 (s, 2H), 9.10 (s, 2H), 9.95 (d, 2H), 10.36 (s, 1H), 11.42 (s, 1H). ^{13}C NMR (DMSO): δ 32.39, 35.89, 36.13, 36.22, 36.31, 41.93, 49.79, 54.43, 54.66, 104.10, 104.72, 118.26, 118.53, 121.35, 122.09, 122.23, 122.38, 122.71, 122.89, 141.30, 150.44, 158.4, 161.51, 162.21, 164.13, 169.25. FAB (EM high resolution) calculated for $C_{31}H_{39}N_{12}O_6Cl_2$ [M - Cl]$^+$: 745.2493. Found: 745.2492. Anal. ($C_{31}H_{39}N_{12}O_6Cl_3$): C, H, Cl, N.

3-[1-Methyl-4-[1-methyl-4-[1-methyl-4-[*N*1-[5-bis(2-chloroethyl)amino-2,4-(1*H*,3*H*)pyrimidinedione]propanoyl-amino]pyrrole-2-carboxamido]pyrrole-2-carboxamido]-pyrrole-2-carboxamido]propionamidine hydrochloride (30): white solid; 630 mg (79% yield); mp 215 °C. ^{1}H NMR (DMSO): δ 2.63 (m, 4H), 3.19 (t, 4H, J = 6.7 Hz), 3.48 (t, 4H, J = 6.7 Hz), 3.56 (t, 2H, J = 6.6 Hz), 3.80 (s, 3H), 3.81 (s, 3H), 3.82 (s, 3H), 3.90 (t, 2H, J = 6.4 Hz), 6.83 (d, 1H), 6.93 (d, 1H), 7.03 (d, 1H), 7.20 (q, 2H), 7.23 (d, 1H), 7.32 (s, 1H), 8.26 (t, 1H, J = 5.4 Hz), 8.82 (s, 2H), 9.09 (s, 2H), 9.93 (s, 2H), 10.16 (s, 1H), 11.36 (s, 1H). ^{13}C NMR (DMSO): δ 32.39, 34.07, 35.87, 36.04, 36.11, 36.17, 41.95, 44.87, 54.44, 54.67, 103.69, 104.71, 104.78, 118.24, 118.50, 120.52, 121.69, 122.11, 122.23, 122.37, 122.67, 122.75, 141.04, 150.01, 158.4, 161.49, 162.04, 166.85, 169.23. FAB (EM high resolution) calculated for $C_{32}H_{41}N_{12}O_6Cl_2$ [M - Cl]$^+$: 759.2649. Found: 759.2645. Anal. ($C_{32}H_{41}N_{12}O_6Cl_3$): C, H, Cl, N.

3-[1-Methyl-4-[1-methyl-4-[1-methyl-4-[*N*1-[5-bis(2-chloroethyl)amino-2,4-(1*H*,3*H*)pyrimidinedione]butanoyl-amino]pyrrole-2-carboxamido]pyrrole-2-carboxamido]-pyrrole-2-carboxamido]propionamidine hydrochloride (31): off-white solid; 560 mg (69% yield); mp 198 °C. ^{1}H NMR (DMSO): δ 1.85 (t, 2H, J = 7.1 Hz), 2.27 (t, 2H, J = 7.1 Hz), 2.66 (t, 2H, J = 6.2 Hz), 3.25 (t, 4H, J = 6.6 Hz), 3.49 (m, 2H, J = 6.1 Hz), 3.57 (t, 4H, J = 6.6 Hz), 3.67 (t, 2H, J = 7 Hz), 3.80 (s, 9H), 6.89 (s, 1H), 6.93 (s, 1H), 7.04 (s, 1H), 7.15 (s, 1H), 7.21 (s, 1H), 7.24 (s, 1H), 7.41 (s, 1H), 8.30 (t, 1H, J = 5.3 Hz), 8.94 (s, 2H), 9.19 (s, 2H), 9.96 (d, 2H), 10.04 (s, 1H), 11.30 (s, 1H). ^{13}C NMR (DMSO): δ 24.71, 32.14, 32.35, 35.82, 36.02, 42.57, 47.13, 54.60, 104.07, 104.84, 118.27, 118.47, 121.20, 121.63, 121.96, 122.11, 122.17, 122.38, 122.69, 140.27, 150.19, 158.47, 161.7, 162.05, 168.68, 169.36. FAB (EM high resolution) calculated for $C_{33}H_{43}N_{12}O_6Cl_2$ $[M - Cl]^+$: 773.2806. Found: 773.2809. Anal. ($C_{33}H_{43}N_{12}O_6Cl_3$): C, H, Cl, N.

3-[1-Methyl-4-[1-methyl-4-[1-methyl-4-[*N*1 [5-bis(2-chloroethyl)amino-2,4 (1*H*,3*H*)pyrimidinedione]pentanoyl-amino]pyrrole-2-carboxamido]pyrrole-2-carboxamido]py-rrole-2-carboxamido]propionamidine hydrochloride (32): white solid; 420 mg (51% yield); mp 186 °C. ^{1}H NMR (DMSO): δ 1.56 (m, 4H), 2.26 (m, 2H), 2.63 (t, 2H, J = 6.5 Hz), 3.26 (t, 4H, J = 6.7 Hz), 3.52 (m, 2H, J = 6.5 Hz), 3.57 (t, 4H, J = 6.7 Hz), 3.65 (t, 2H, J = 6.3 Hz), 3.81 (m, 9H), 6.88 (s, 1H), 6.94 (s, 1H), 7.04 (s, 1H), 7.16 (s, 1H), 7.19 (s, 1H), 7,23 (s, 1H), 7.43 (s, 1H), 8.26 (t, 1H, J = 5.7 Hz), 8.75 (s, 2H), 9.05 (s, 2H), 9.92 (m, 3H), 11.31 (s, 1H). ^{13}C NMR (DMSO): δ 22.04, 28.00, 32.40, 34.96, 35.77, 35.99, 42.51, 47.12, 54.48, 103.88, 104.61, 118.02, 118.12, 118.38, 121.07, 121.93, 122.04, 122.14, 122.27, 122.58, 140.16, 150.08, 158.37, 161.39, 161.97, 169.06. FAB (EM high resolution) calculated for $C_{34}H_{45}N_{12}O_6Cl_2$ [M − Cl]$^+$: 787.2962. Found: 787.2964. Anal. ($C_{34}H_{45}N_{12}O_6Cl_3$): C, H, Cl, N.

3-[1-Methyl-4-[1-methyl-4-[1-methyl-4-[*N*1-[5-bis(2-chloroethyl)amino-2,4-(1*H*,3*H*)pyrimidinedione]hexanoyl-amino]pyrrole-2-carboxamido]pyrrole-2-carboxamido]-pyrrole-2-carboxamido]propionamidine hydrochloride (33): off-white solid; 545 mg (65% yield); mp 180 °C. ^{1}H NMR (DMSO): δ 1.30 (m, 2H), 1.57 (m, 4H), 2.23 (t, 2H, J = 7.1 Hz), 2.63 (t, 2H, J = 6.7 Hz), 3.26 (t, 4H, J = 6.5 Hz), 3.50 (m, 2H), 3.56 (t, 4H, J = 6.4 Hz), 3.62 (m, 2H), 3.80 (s, 3H), 3.81 (s, 3H), 3.83 (s, 3H), 6.88 (s, 1H), 6.94 (s, 1H), 7.05 (s, 1H), 7.16 (s, 1H), 7.20 (s, 1H), 7.24 (s, 1H), 7.43 (s, 1H), 8.26 (t, 1H,

J = 5.2 Hz), 8.78 (s, 2H), 9.07 (s, 2H), 9.88 (s, 1H), 9.94 (d, 2H), 11.29 (s, 1H). ^{13}C NMR (DMSO): δ 25.00, 25.50, 28.22, 32.46, 35.45, 35.85, 36.06, 42.64, 47.35, 54.63, 104.04, 104.74, 118.10, 118.22, 118.47, 121.07, 122.06, 122.12, 122.21, 122.38, 122.70, 140.44, 150.00, 158.47, 161.48, 161.9, 169.20, 169.35. FAB (EM high resolution) calculated for $C_{35}H_{47}N_{12}O_6Cl_2$ [M − Cl]$^+$: 801.3119. Found: 801.3115. Anal. ($C_{35}H_{47}N_{12}O_6Cl_3$): C, H, Cl, N.

3-[1-Methyl-4-[1-methyl-4-[1-methyl-4-[*N*1-[5-bis(2-chloroethyl)amino-2,4-(1*H*,3*H*)pyrimidinedione]heptanoylamino]pyrrole-2-carboxamido]pyrrole-2-carboxamido]-pyrrole-2-carboxamido]propionamidine hydrochloride (34): white solid; 535 mg (63% yield); mp 94 °C. ^{1}H NMR (DMSO): δ 1.26 (m, 4H), 1.54 (m, 4H), 2.21 (t, 2H, J = 7.2 Hz), 2.61 (t, 2H, J = 6.4 Hz), 3.25 (t, 4H, J = 6.5 Hz), 3.49 (m, 2H), 3.58 (t, 4H, J = 6.5 Hz), 3.61 (t, 2H, J = 6.9 Hz), 3.80 (s, 3H), 3.81 (s, 3H), 3.83 (s, 3H), 6.87 (s, 1H), 6.94 (s, 1H), 7.04 (s, 1H), 7.14 (s, 1H), 7.18 (s, 1H), 7.22 (s, 1H), 7.41 (s, 1H), 8.24 (t, 1H, J = 5.6 Hz), 8.69 (s, 2H), 9.01 (s, 2H), 9,83 (s, 1H), 9.92 (s, 1H), 9.93 (s, 1H), 11.29 (s, 1H). ^{13}C NMR (DMSO): δ 25.33, 25.67, 28.32, 28.40, 32.58, 35.53, 35.88, 36.12, 42.67, 47.44, 54.60, 104.01, 104.71, 118.13, 118.21, 118.48, 120.97, 122.08, 122.15, 122.25, 122.37, 122.65, 122.68, 140.59, 150.19, 158.47, 161.50, 162.09, 169.11, 169.46. FAB (EM high resolution) calculated for $C_{36}H_{48}N_{12}O_6NaCl_2$ [M − HCl + Na]$^+$: 837.3094. Found: 837.3093. FAB (EM high resolution) calculated for $C_{36}H_{49}N_{12}O_6Cl_2$ [M − Cl]$^+$: 815.3275. Found: 815.3274. Anal. ($C_{36}H_{49}N_{12}O_6Cl_3$): C, H, Cl, N.

Cytotoxicity Assay. The K562 human chronic myeloid leukemia cells were maintained in RPM1 1640 medium supplemented with 10% fetal calf serum and 2 mM glutamine at 37 °C in a humidified atmosphere containing 5% CO_2 and were incubated with a specified dose of drug for 1 h at 37 °C in the dark. The incubation was terminated by centrifugation (5 min, 300*g*), and the cells were washed once with drug-free medium. Following the appropriate drug treatment, the cells were transferred to 96-well microtiter plates, with 10^4 cells per well and 8 wells per sample. Plates were then kept in the dark at 37 °C in a humidified atmosphere containing 5% CO_2. The assay is based on the ability of viable cells to reduce a yellow soluble tetrazolium salt, 3-(4,5-dimethylthiazol-2-yl)-2,5-diphenyl-2*H*-tetrazolium bromide (MTT, Sigma Chemical Co.) to an insoluble purple formazan precipitate. Following incubation of the plates for 4 days (to allow control cells to increase in number by 10-fold), 20 μL of a 5 mg/mL solution of MTT in phosphate-buffered saline was added to each well and the plates were further incubated for 5 h. The plates were then centrifuged for 5 min at 300*g*, and the bulk of the medium was pipetted from the cell pellet, leaving 10−20 μL per well. A total of 200 μL of DMSO was added to each well, and the samples were agitated to ensure complete mixing. The optical density was then read at a wavelength of 550 nm on a Titertek Multiscan ELISA plate reader, and the dose−response curve was constructed. For each curve, an IC_{50} value was read as the dose required to reduce the final optical density to 50% of the control value.

Taq DNA Polymerase Stop Assay.[38a] Plasmid pUC18 DNA was linearized with HindIII to provide a stop for the Taq downstream from the primer. The oligodeoxynucleotide primer (5′CTCACTCAAAGGCGGTAATAC) was 5′-end-labeled prior to amplification using T4 polynucleotide kinase and [γ-^{32}P]-ATP (5000 Ci/mmol, Amersham, U.K.). The labeled primers were purified by elution through Bio-Rad spin columns. Linear amplification of DNA was carried out in a total volume of 100 μL containing 0.5 μg of template DNA, 5 pmol of labeled primer, 200 μM of each dNTP, 10 U of Taq polymerase, 50 mM KCl, 10 mM Tris-HCl, pH 9.0, 0.1% Triton X-100, 2.5 mM $MgCl_2$. Where appropriate, template DNA reacted with the test agent for 1 h at 37 °C and then precipitated with ethanol. After an initial denaturation at 94 °C for 4 min, the cycling conditions were as follows: 94 °C for 1 min, 60 °C for 1 min, and 72 °C for 1 min, for a total of 30 cycles. After being amplified, the samples were ethanol-precipitated and washed with 70% ethanol. Samples were dissolved in formamide loading dye, heated for 2 min at 90 °C, cooled on ice, and electrophoresed at 2500−3000 V for 3 h on a 80 cm × 20 cm × 0.4 mm 6% acrylamide denaturing sequencing gel (Sequagel, National Diagnostics). The gels were dried, and X-ray film was exposed to the gels (Hyperfilm, Amersham, U.K.).

Thermal Cleavage Assay.[38b] A 208 base pair 5′-singly-end-labeled fragment was generated by PCR from HindIII linearized pUC18 using 5′-end-labeled primer TGGTATCTT-TATAGTCCTGTCG and unlabeled primer 5′-CTCACTCAAAG-GCGGTAATAC. Labeled DNA reacted with the test compound for 1 h at 37 °C and was ethanol-precipitated, washed, dried, and resuspended in 100 μL of 1.5 mM sodium citrate and 15 mM NaCl. Thermal cleavage was at 90 °C for 30 min. Samples were ethanol-precipitated and resuspended in formamide loading dye and electrophoresed as for the Taq polymerase stop assay.

Molecular Modeling Studies. Molecular modeling of the distamycin hybrids was performed using the SYBYL molecular modeling package.[39] Three DNA sequences have been studied. In the first, with the object of testing the force field and the optimization procedure, an experimental X-ray three-dimensional structure of distamycin complexed[40] with a DNA dodecamer 5′-CGCAAATTTGCG-3′ was obtained from the RCSB Protein Data Bank (http://www.rcsb.org) and used as the starting geometry.

To reproduce the footprinting results obtained for compounds **29**−**34**, the study of two new types of complexes was accomplished with base sequences of 5′-TCGATTTTTGTGAT-3′ and 5′-GGCCTTTTTACGGT-3′, respectively.

In the first sequence, all hydrogen atoms were added to both the DNA double strand and the ligand. DNA atomic charges were read from the Kollman all-atoms dictionary implemented in SYBYL, and distamycin charges were calculated with an AM1[41,42] Hamiltonian implemented in MOPAC,[43] using a protonated guanidium moiety model. Geometry was optimized using the Powell[44] method and the Tripos force field[45] (ϵ = 1, distance-dependent) until the gradient was smaller than 0.1 kcal mol^{-1} Å^{-2}. This optimized distamycin complex shows the described hydrogen bond pattern[7] formed between the NH moieties of the ligand and the adenine N3 and thymine O2 atoms and was used for the subsequent stages.

The two new DNA double strands were built from standard fragments and superimposed onto the appropriate base pairs of the first complex with the object of situating the distamycin in an adequate orientation inside the minor groove of both new DNA double strands. Both complexes were optimized using the previously describe procedure. This study shows that distamycin binds to both DNA sequences in a way similar to that of the experimentally described first sequence.[7] Once the three DNA−distamycin complexes have been optimized, a study of complexes between the three DNA sequences and compounds **29**−**34** was completed.

Distamycin was extracted from each complex, and the new hybrids were built by addition of the appropriate standard fragments. MOPAC charges were calculated, and a partial minimization of each new ligand was performed, keeping rigid the distamycin moiety in order to relax steric interactions without losing the bowed shape of distamycin. The minimized ligands were inserted into the minor groove of each DNA sequence, and the whole complex was optimized again using the conditions described above.

To investigate the more favored conformations of the ligands into the DNA, a conformational search was performed, rotating all the bonds of the fragments added to distamycin in each new hybrid. The 50 most stable conformations of each search were selected and minimized, and their structures were carefully studied.

Acknowledgment. We thank Pharmacia & Upjohn for providing distamycin A, and we thank Ministero Università e Ricerca Scientifica (MURST) (60%) and The Cancer Research Compaign (U.K.) for financial support of this work.

References

(1) Turner, P. R.; Denny W. A. The mutagenic properties of DNA minor-groove binding ligands. *Mutat. Res.* **1996**, *355*, 141−169.

(2) Hartley, J. A.; Lown, J. W.; Mattes, W. B.; Kohn, K. W. DNA sequence specificity of antitumor agents. Oncogenes as possible targets for cancer therapy. *Acta Oncol.* **1998**, *27*, 503−510.

(3) Dervan, P. B. DNA-binding molecules. *Science* **1986**, *232*, 464−471.

(4) Arcamone, F.; Orezzi, P. G.; Barbieri, W.; Nicolella, V.; Penco, S. Distamycin A. Isolation and structures of the antiviral agent distamycin A. *Gazz. Chim. Ital.* **1967**, *97*, 1097−1115.

(5) Arcamone, F.; Di Marco, A.; Gaetani, M.; Scotti, T. Isolation and antitumor activity of an antibiotic from *Streptomyces*. *G. Microbiol.* **1961**, *9*, 83−90.

(6) Arcamone, F.; Penco, S.; Orezzi, P. G.; Nicolella, V.; Pirelli, A. Structure and synthesis of distamycin A. *Nature* **1964**, *203*, 1064−1065.

(7) Pelton, J. G.; Wemmer, D. E. Binding modes of distamycin A with d(CGCAAATTTGCG)2 determined by two-dimensional NMR. *J. Am. Chem. Soc.* **1990**, *112*, 1393−1399.

(8) Abu-Daya, A.; Brown, P. M.; Fox, K. R. DNA sequence preferences of several AT-selective minor groove binding ligands. *Nucleic Acids Res.* **1995**, *23*, 3385−3392. Pelton, J. C.; Wemmer, D. E. Structural modeling of the distamycin A. d(CGCGAATTCGCG)$_2$ complex 2D NMR and molecular mechanics. *Biochemistry* **1988**, *27*, 8088−8096.

(9) Coll, M.; Frederick, C. A.; Wang, A. H.; Rich, A. A bifurcated hydrogen-bonded conformation in the d(A,T) base pairs of the DNA dodecamer d(CGCAAATTTGCG) and its complex with distamycin. *Proc. Natl. Acad. Sci. U.S.A.* **1987**, *84*, 8385−8389.

(10) Kopka, M. L.; Yoon, C.; Goodsell, D.; Pjura, P.; Dickerson, R. E. The molecular origin of DNA−drug specificity in netropsin and distamycin. *Proc. Natl. Acad. Sci. U.S.A.* **1985**, *82*, 1376−1380.

(11) Cozzi, P.; Mongelli, N.; Cytotoxics derived from distamycin A and congeners. *Curr. Pharm. Des.* **1998**, *4*, 181−201.

(12) Marchini, S.; Broggini, M.; Sessa, C.; D'Incalci, M. Development of distamycin-related DNA binding anticancer drugs. *Expert Opin. Invest. Drugs* **2001**, *10*, 1703−1714.

(13) Zunino, F.; Animati, F.; Capranico, G. DNA minor-groove binding drugs. *Curr. Pharm. Des.* **1995**, *1*, 83−94.

(14) Baraldi, P. G.; Cacciari, B.; Spalluto, G.; Romagnoli, R. DNA Minor Groove Alkylating Agents Structurally Related to Distamycin A. *Expert Opin. Ther. Pat.* **2000**, *6*, 891−904.

(15) Kennedy, B. J.; Torkelson, J. L.; Torlakovic, E. Uracil mustard revised. *Cancer* **1999**, *85*, 2265−2272.

(16) Berry, D. H.; Sutow, W. W.; Vietti, T. J.; Fernbach, D. J.; Sullivan, M. P.; Haggard, M. E.; Lane, D. M. Evaluation of uracil mustard in children with Hodkin's disease, lymphosarcoma and soft tissue sarcoma. *J. Clin. Pharmacol. New Drugs* **1972**, *12*, 169−173.

(17) Fernbach, D. J.; Haddy, T. B.; Holcomb, T. M.; Lusher, J.; Sutow, W. W.; Vietti, T. J. Uracil mustard (NSC-34462) therapy for children with metastatic neuroblastoma. *Cancer Chemother. Rep.* **1968**, *52*, 287−291.

(18) Sokal, J. E. Current concepts in the treatment of chronic myelocytic leukemia. *Cancer* **1972**, *30*, 1275−1278.

(19) Robertson, J. H. Uracil mustard in the treatment of thrombocytemia. *Blood* **1970**, *35*, 288−297.

(20) Doweyko, A. M.; Mattes, W. B. An application of 3D-QSAR to the analysis of the sequence specificity of DNA alkylation by uracil mustard. *Biochemistry* **1992**, *31*, 9388−9392.

(21) Hartley, J. A.; Bingham, J. P.; Souhami, R. L. DNA sequence selectivity of guanine-N7 alkylation by nitrogen mustards is preserved in intact cells. *Nucleic Acids Res.* **1992**, *20*, 3175−3178.

(22) Mattes, W. B.; Hartley, J. A.; Kohn, K. W. DNA sequence selectivity of guanine-N7 alkylation by nitrogen mustards. *Nucleic Acids Res.* **1986**, *14*, 2971−2987.

(23) Baiily, C.; Hènichart, J. Molecular pharmacology of intercalator−minor groove binder hybrid molecules. In *Molecular Aspects of Anticancer Drug−DNA Interactions*; Neidle, S., Waring, M. J., Eds.; Mcmillan: London, 1994; Vol. 2, pp 162−196.

(24) Sondhi, S. M.; Praveen Reddy, B. S.; Lown, J. W. Lexitropsin conjugates: action on DNA targets. *Curr. Med. Chem.* **1997**, *4*, 313−358.

(25) Xie, Y.; Miller, G. G.; Cubitt, S. A.; Soderlind, K. J.; Allalunis-Turner, M. J.; Lown, J. W. Enediyne-lexitropsin DNA-targeted anticancer agents. Physicochemical and cytotoxic properties in human neoplastic cells in vitro, and intracellular distribution. *Anti-Cancer Drug Des.* **1997**, *12*, 169−179.

(26) Bailly, C.; Pommery, N.; Houssin, R.; Henichart, J. P. Design, synthesis, DNA binding, and biological activity of a series of DNA minor-groove binding intercalating drugs. *J. Pharm. Sci.* **1989**, *78*, 910−917.

(27) Riou, J. F.; Grondard, L.; Naudin, A.; Bailly, C. Effects of two distamycin−ellipticine hybrid molecules on topoisomerase-I and topoisomerase-II mediated DNA cleavage−relation to cytotoxicity. *Biochem. Pharmacol.* **1995**, *50*, 424−428.

(28) Helissey, P.; Bailly, C.; Vishwakarma, J. N.; Auclair, C.; Waring, M. J.; Giorgi-Renault, S. DNA minor groove cleaving agents: synthesis, DNA binding and DNA cleaving properties of anthraquinone−oligopyrrolecarboxamide hybrids. *Anti-Cancer Drug Des.* **1996**, *11*, 527−551.

(29) Satz, A. L.; Bruice, T. C. Recognition of nine base pairs in the minor groove of DNA by a tripyrrole peptide−Hoechst conjugate. *J. Am. Chem. Soc.* **2001**, *123*, 2469−2477.

(30) Baraldi, P. G.; Cacciari, B.; Guiotto, A.; Romagnoli, R.; Spalluto, G.; Mongelli, N.; Thurston, D. E.; Howard, P. W.; Leoni, A.; Bianchi, N.; Gambari, R. Design, synthesis and biological activity of pyrrolo[2,1-*c*][1,4]benzodiazepine (PBD)−distamycin hybrid. *Bioorg. Med. Chem. Lett.* **1998**, *8*, 3019−3024.

(31) Baraldi, P. G.; Cacciari, B.; Guiotto, A.; Manfredini, S.; Romagnoli, R.; Spalluto, G.; Thurston, D. E.; Bianchi, N.; Rutigliano, C.; Mischiati, C.; Gambari, R. Synthesis, Antiproliferative Activity, and DNA-Binding Properties of Hybrid Molecules Containing Pyrrolo[2,1-*c*][1,4]benzodiazepine (PBD) and Minor Groove Binding Oligopyrrole Carriers. *J. Med. Chem.* **1999**, *42*, 5131−5141.

(32) Damayanthi, Y.; Praveen Reddy, B. S.; Lown, J. W. Design and synthesis of novel pyrrolo[2,1-*c*][1,4]benzodiazepine−lexitropsin conjugates. *J. Org. Chem.* **1999**, *64*, 290−292.

(33) Praveen Reddy, B. S.; Damayanthi, Y.; Narayan Reddy, B. S.; Lown, J. W. Design, synthesis and in vitro cytotoxicity studies of novel pyrrolo[2,1-*c*][1,4]benzodiazepine (PBD)−polyamide conjugates and 2,2′-PBD dimers. *Anti-Cancer Drug Des.* **2000**, *15*, 225−238.

(34) Fregeau, N. L.; Wang, Y.; Pon, R. T.; Wylie, W. A.; Lown, J. W. Characterization of a CPI−Lexitropsin conjugate−oligonucleotide covalent complex by ^{1}H NMR and restrained molecular dynamics simulation. *J. Am. Chem. Soc.* **1995**, *117*, 8917−8925.

(35) Wang, Y.; Gupta, R.; Huang, L.; Luo, W.; Lown, J. W. Design, synthesis, cytotoxic properties and preliminary DNA sequencing evaluation of CPI−*N*-methylpyrrole hybrids. Enhancing effect of a trans double bond linker and role of terminal amide functionality on cytotoxic potency. *Anti-Cancer Drug Des.* **1996**, *11*, 15−34.

(36) Baraldi, P. G.; Balboni, G.; Pavani, M. G.; Spalluto, G.; Tabrizi, M. A.; De Clercq, E. D.; Balzarini, J.; Bando, T.; Sugiyama, H.; Romagnoli, R. Design, synthesis, DNA binding, and biological evaluation of water-soluble hybrid molecules containing two pyrazole analogues of the alkylating cyclopropylpyrroloindole (CPI) subunit of the antitumor agent CC-1065 and polypyrrole minor groove binders. *J. Med. Chem.* **2001**, *44*, 2536−2543.

(37) Martinez, A. P.; Lee, W. W.; Goodman, L. Nitrogen mustards derived from 3,4-dihydro-2,4-dioxo-1(2*H*)-pyrimidinepropionic and butyric acids. *J. Med. Chem.* **1965**, 187−189.

(38) (a) Ponti, M.; Forrow, S. M.; Souhami, R. L.; D'Incalci, M.; Hartley, J. A. Measurement of the sequence specificity of covalent DNA modification by antineoplastic agents using Taq DNA polymerase. *Nucleic Acids Res.* **1991**, *19*, 2929−2933. (b) Hartley, J. A.; Wyatt, M. D. Determination of the sequence specificity of alkylation damage using cleavage-based assays. In *Methods in Molecular Biology*; *Drug−DNA Interaction Protocols*; Fox, K., Ed.; Humana Press: Totowa, NJ, 1997; Vol. 90, pp147−156.

(39) SYBYL Molecular Modeling Software: Tripos Inc., 1699 S. Hanley Road; St. Louis, MO 63144-2913, http://www.tripos.com.

(40) Coll, M.; Frederick, C. A.; Wang, A. H.; Rich, A. A bifurcated hydrogen-bonded conformation in the d(A.T) base pairs of the DNA dodecamer d(CGCAAATTTGCG) and its complex with distamycin. *Proc. Natl. Acad. Sci. U.S.A.* **1987**, *84*, 8385−8389.

(41) Dewar, M. J. S.; Zoebisch, E. G.; Healy, E. F.; Stewart, J. J. P. AM1: a new general purpose quantum mechanical molecular model. *J. Am. Chem. Soc.* **1985**, *107*, 3902−3909.

(42) Dewar M. J. S.; Zoebisch, E. G. Extension of AM1 to the halogens. *THEOCHEM* **1988**, *180*, 1.

(43) Stewart, J. J. MOPAC: A Semiempirical Molecular Orbital Program. *J. Comput.-Aided Mol. Des.* **1990**, *4*, 1−105.

(44) Powell, M. J. D. Restart procedures for the conjugate gradient mMethod. *Math. Programming* **1997**, *12*, 241−254.

(45) Clark, M.; Cramer, R. D.; Van Opdenbosch, N. Validation of the general purpose Tripos 5.2 force field. *J. Comput. Chem.* **1989**, *10*, 982−1012.

JM011113B